



## Rational synthetic strategy: From ZnO nanorods to ZnS nanotubes

Ran Yi<sup>a</sup>, Guanzhou Qiu<sup>a</sup>, Xiaohe Liu<sup>a,b,\*</sup>

<sup>a</sup> Department of Inorganic Materials, Central South University, Changsha, Hunan 410083, People's Republic of China

<sup>b</sup> State Key Laboratory of Powder Metallurgy, Central South University, Changsha, Hunan 410083, People's Republic of China

### ARTICLE INFO

#### Article history:

Received 13 June 2009

Received in revised form

20 July 2009

Accepted 22 July 2009

Available online 30 July 2009

#### Keywords:

ZnO

ZnS

Core/shell structures

Nanotubes

Optical properties

### ABSTRACT

We demonstrate here that ZnS nanotubes can be successfully synthesized via a facile conversion process from ZnO nanorods precursors. During the conversion process, ZnO nanorods are first prepared as sacrificial templates and then converted into tubular ZnO/ZnS core/shell nanocomposites through a hydrothermal sulfidation treatment by using thioacetamide (TAA) as sulfur source. ZnS nanotubes are finally obtained through the removal of ZnO cores of tubular ZnO/ZnS core/shell nanocomposites by KOH treatment. The photoluminescence (PL) characterization of the as-prepared products shows much enhanced PL emission of tubular ZnO/ZnS core/shell nanocomposites compared with their component counterparts. The probable mechanism of conversion process is also proposed based on the experimental results.

© 2009 Elsevier Inc. All rights reserved.

### 1. Introduction

During the past decades, wide band gap semiconductor materials have attracted considerable attention due to their size-dependent properties and important technological applications. In particular, ZnS is one of the important semiconductor materials with a wide band gap of 3.7 eV and received a wide range of research interest because of its potential applications in various fields such as nonlinear optical devices, displays, sensors, infrared windows, and lasers [1–3]. Various synthetic routes, for example, solvothermal procedure, hydrothermal method, solid–vapor deposition technique, pulsed laser vaporization [4–6], have been employed to prepare ZnS with different morphologies like nanobelts, nanorods, nanowires, nanoribbons, hollow nanospheres, and other hierarchical nanostructures [7–12]. Recently, a new approach to the preparation of ZnS and ZnS nanocomposites with various morphologies based on corresponding ZnO precursors has been a focus of materials research. Hexagonal ZnS nanotubes have been obtained via a conversion and etching process of ZnO nanocolumns [13]. ZnO/ZnS nanocable and ZnS nanotube arrays have been successfully synthesized by a thioglycolic acid-assisted solution route with removal of ZnO cores [14] and by the conversion from ZnO nanorods due to the Kirkendall effect under simple ultrasonic irradiation [15],

respectively. ZnO/ZnS core/shell microspheres have been prepared with ZnO microspheres as reactive templates and they exhibit a distinct enhancement of photoluminescence compared with the uncoated ZnO microspheres [16]. ZnS hollow nanospheres with nanoporous shell were successfully synthesized through the evolution of ZnO nanospheres [12]. Heterostructured ZnO/ZnS core/shell nanotube arrays were synthesized by a conversion process from ZnO nanorod arrays grown by atomic-layer deposition [17]. The examples above are generally two-step routes while there are still other reports on one-pot process in which ZnO precursors were not point out by the authors but the conversion from ZnO to ZnS was most likely one of the growth mechanisms. For example, hollow ZnS microspheres [18], bifunctional ZnO/ZnS nanoribbons decorated by  $\gamma$ -Fe<sub>2</sub>O<sub>3</sub> clusters [19], and flowerlike ZnS–ZnO heterogeneous microstructures built up by ZnS-particle-strewn ZnO microrods [20]. However, there are few reports of tubular ZnO/ZnS core/shell nanocomposites and ZnS nanotubes using ZnO nanorods precursors via a hydrothermal route.

In this paper, tubular ZnO/ZnS core/shell nanocomposites could be successfully obtained via a sulfidation conversion by using ZnO nanorods as sacrificial templates in which thioacetamide (TAA) was used as sulfur source. ZnS nanotubes could also be successfully obtained via an alkali treatment process of tubular ZnO/ZnS core/shell nanocomposites. Compared with ZnO nanorods, as-prepared ZnO/ZnS core/shell nanocomposites and ZnS nanotubes exhibit much different room-temperature photoluminescence (PL) properties. The possible formation mechanism of tubular ZnO/ZnS core/shell nanocomposites was also proposed. This strategy may provide more opportunities for the preparation of core/shell structured and hollow metal chalcogenides.

\* Corresponding author at: Department of Inorganic Materials, Central South University, Changsha, Hunan 410083, People's Republic of China. Fax: +86 731 8879815.

E-mail address: liuxh@mail.csu.edu.cn (X. Liu).

## 2. Experimental section

All chemicals were of analytical grade from Shanghai Chemical Reagents Co., and used as starting materials without further purification.

### 2.1. Preparation of ZnO nanorods

In a typical procedure, 0.297 g of  $\text{Zn}(\text{NO}_3)_2 \cdot 6\text{H}_2\text{O}$  and 0.142 g of  $\text{Na}_2\text{SO}_4$  were loaded into a Teflon-lined stainless steel autoclave of 50 ml capacity and dissolved in 30 ml deionized water. Then 5.0 ml of hydrazine monohydrate (80% v/v) solution was added dropwise during vigorous stirring. Next, the autoclave was filled with deionized water up to 80% of the total volume, after 10 min stirring, sealed and maintained at 180 °C for 24 h. Subsequently, the system was allowed to cool to room temperature naturally. The resulting precipitate was collected by filtration and washed with absolute ethanol and distilled water in sequence for several times. The final product was dried in a vacuum box at 50 °C for 4 h.

### 2.2. Preparation of tubular ZnO/ZnS core/shell nanocomposites

ZnO nanorods (0.081 g) and thioacetamide (TAA, 0.075 and 0.75 g, respectively) were put into a Teflon-lined stainless steel autoclave of 50 ml capacity and dissolved in 30 ml deionized water. The solution was stirred vigorously for 10 min and sealed and maintained at 100 °C for 6 h, and then cooled down to room temperature. The resulting precipitate was collected by filtration and washed with absolute ethanol and distilled water in sequence for several times. The final product was dried in a vacuum box at 50 °C for 4 h.

### 2.3. Preparation of ZnS nanotubes

Tubular ZnO/ZnS core/shell nanocomposites (0.01 g) were soaked in KOH solution (4 mol/l) under constant stirring for 1 h at room temperature. Finally, the obtained products were collected by centrifugation and washed with distilled water repeatedly and then dried in vacuum box at 50 °C for 4 h.

### 2.4. Characterization

The obtained products were characterized on a D/max2550 VB+X-ray powder diffractometer (XRD) with  $\text{CuK}\alpha$  radiation ( $\lambda = 1.54178 \text{ \AA}$ ). The operation voltage and current were kept at 40 kV and 40 mA, respectively. The size and morphology of the as-synthesized products were determined at 20 kV by a XL30 S-FEG scanning electron microscope (SEM) and at 160 kV by a JEM-200CX transmission electron microscope (TEM) and a JEOL JEM-2010F high-resolution transmission electron microscope (HRTEM). Energy-dispersive X-ray spectroscopy (EDS) was taken on the SEM. The room-temperature photoluminescence (PL) measurement was carried out on an F-2500 spectrophotometer using the 325 nm excitation line of Xe light. ZnO nanorods, ZnO/ZnS core/shell nanocomposites and ZnS nanotubes powder were used as the standards. UV–Vis absorption spectra (UV–Vis) were performed on a Perkin-Elmer Lambda-20 spectrometer at room temperature. For UV spectroscopic analysis samples were dispersed thoroughly in distilled water.

## 3. Results and discussion

The crystal structure and crystallinity of the as-prepared products were investigated by XRD. Fig. 1(a) shows a typical

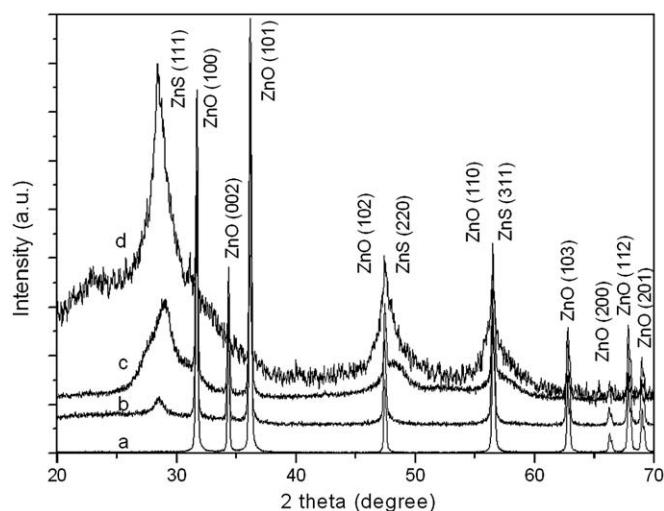


**Fig. 1.** XRD patterns of the as-prepared ZnO nanorods (a), tubular ZnO/ZnS core/shell nanocomposites obtained with different molar ratios of ZnO to TAA: (b) 1:1, (c) 1:10, and ZnS nanotubes (d).

XRD pattern of ZnO precursors, in which all the diffraction peaks can be well indexed to hexagonal ZnO with lattice constants  $a = 3.249 \text{ \AA}$  and  $c = 5.208 \text{ \AA}$ , in good agreement with the standard PDF data (JCPDS file 36–1451). The XRD patterns of tubular ZnO/ZnS core/shell nanocomposites prepared with different molar ratios of ZnO to TAA were shown in Fig. 1(b) and (c), respectively. Besides those of ZnO, characteristic diffraction peaks corresponding to face-centered cubic ZnS can be observed after the sulfidation treatment of ZnO precursors, indicating the formation of ZnO/ZnS nanocomposites. The intensity of main diffraction peaks of ZnS in Fig. 1(c) is much stronger than that in Fig. 1(b), showing more ZnS was formed after sulfidation treatment due to the larger molar ratio of ZnO to TAA. Fig. 1(d) shows the XRD patterns of ZnS nanotubes obtained via an alkali treatment process of tubular ZnO/ZnS core/shell nanocomposites (Fig. 1(c)). The main diffraction peaks in the pattern can be indexed as the face-centered cubic ZnS with lattice constants  $a = 5.406 \text{ \AA}$  (space group:  $F\bar{4}3m(216)$ ), which are consistent with the values in the literature (JCPDS file 05-0566). The average nanocrystallite size of ZnS products is estimated to be about 2.8 nm by employing the well-known Debye–Scherrer formula, close to exciton Bohr radius of ZnS (about 2.5 nm) [21].

The morphology, structure, and size of ZnO nanorods were characterized with SEM, TEM and HRTEM. Fig. 2(a) and (b) shows typical low and high magnification SEM images of ZnO precursors, respectively, in which large quantities of ZnO nanorods with diameter in the range of 100–800 nm and length up to 10  $\mu\text{m}$  can be clearly observed. EDS analysis (Fig. S1 of supporting materials) exhibits the products only consist of Zn and O in addition to C which is caused by the C substrate, consistent with XRD characterization. Fig. 2(c) is a representative TEM image of ZnO nanorods, which shows the morphology of several nanorods is relatively straight. Detailed information regarding to the crystal structure of final products has been investigated by HRTEM. Fig. 2(d) shows a typical HRTEM image of an individual ZnO nanorod. The lattice spacing was calculated to be 0.52 nm, corresponding to the  $d$ -spacing of (0001) crystal plane of the wurtzite ZnO, which suggests that those nanorods are single crystalline and grow along the [0001] direction. The inset of Fig. 2(d) is the corresponding fast Fourier transform (FFT) image of HRTEM result, showing that the nanorod is of single-crystalline structure with preferential [0001] growth direction.

Download English Version:

<https://daneshyari.com/en/article/1330963>

Download Persian Version:

<https://daneshyari.com/article/1330963>

[Daneshyari.com](https://daneshyari.com)